Detection of rank-P signals in Cognitive Radio Networks with uncalibrated multiple antennas

David Ramírez, *Student Member, IEEE,* Gonzalo Vazquez-Vilar, *Student Member, IEEE,*
Roberto López-Valcarce, *Member, IEEE,* Javier Vía, *Member, IEEE,*
and Ignacio Santamaría, *Senior Member, IEEE*

***Abstract*—Spectrum sensing is a key component of the Cognitive Radio paradigm. Typically, primary signals have to be detected with uncalibrated receivers at signal-to-noise ratios (SNRs) well below decodability levels. Multiantenna detectors exploit spatial independence of receiver thermal noise to boost detection performance and robustness. We study the problem of detecting a Gaussian signal with rank-P unknown spatial covariance matrix in spatially uncorrelated Gaussian noise with unknown covariance using multiple antennas. The generalized likelihood ratio test (GLRT) is derived for two scenarios. In the first one, the noises at all antennas are assumed to have the same (unknown) variance, whereas in the second, a generic diagonal noise covariance matrix is allowed in order to accommodate calibration uncertainties in the different antenna frontends. In the latter case, the GLRT statistic must be obtained numerically, for which an efficient method is presented. Furthermore, for asymptotically low SNR, it is shown that the GLRT does admit a closed form, and the resulting detector performs well in practice. Extensions are presented in order to account for unknown temporal correlation in both signal and noise, as well as frequency-selective channels.**

I. Introduction

Cognitive Radio (CR) has the potential to improve wireless spectrum usage and alleviate the apparent scarcity of spectral resources as seen today [1], [2]. The key idea behind CR is to allow opportunistic access to temporally and/or geographically unused licensed bands. Thus, spectrum sensing constitutes a key component in CR, in order to identify vacant channels and avoid interference to rightful license owners [3].

The wireless medium makes reliable detection of these users a very challenging task: due to fading and shadowing phenomena, the received primary signal may be very weak, resulting in very low signal-to-noise ratio (SNR) operation conditions [4]. Any structure in the primary signal, such as the presence of pilots or cyclostationary features, could, in principle, be exploited for detection purposes. However, most such approaches require some level of synchronization with the primary signal, which cannot be guaranteed in very low SNRs [4]. In order to avoid these drawbacks, asynchronous detectors can be considered. The simpler asynchronous detectors, including the popular energy detector, require knowledge of the noise variance in order to compute the detection threshold. Any uncertainty regarding this parameter translates in severe performance degradation, so that the detection/false alarm requirements may not be satisfied [5].

This serious drawback motivates the search for asynchronous detectors robust to noise uncertainty, one possibility being the use of multiple–antenna sensors. Several authors have explored this strategy in order to enhance detection performance in the context of CR systems. Assuming a temporally white Gaussian model for both signal and noise, spatially white noise with unknown variance across antennas, and an unknown rank-1 spatial covariance matrix for the signal, several detectors have been proposed [6]–[12].

However, in practical scenarios, the spatial rank of the received signals may be larger than one. This is the case, for example, if multiple independent users (e.g. from adjacent cells) simultaneously access the same frequency channel. Alternatively, many state-of-the-art communication standards consider the simultaneous transmission of different data streams through multiple antennas to achieve multiplexing gain and/or the use of space-time codes to enhance spatial diversity. For these systems, the signal received at the multiantenna sensor will exhibit a spatial rank equal to the number of independent streams or the spatial size of the code, respectively. Examples range from broadcasting standards, such as the european DVB-T2 [13] which considers 2-antenna space-time Alamouti codes, to point-to-multipoint standards, such as IEEE 802.11n [14], IEEE 802.16 [15] or LTE [16], which support up to four transmit antennas. Hence, it is of interest to develop detectors for signals with spatial rank $P > 1$.

We focus on the generalized likelihood ratio test (GLRT) for the detection of vector-valued rank-P signals when the noise covariance matrix is unknown. In particular the contributions of this paper are:

1) We derive the GLRT for vector-valued rank-P signals and independent, identically distributed (iid) noises at each antenna when both signal and noise are assumed temporally white.
2) We formulate the GLRT for a similar scenario, but with the noise components having different (unknown)

D. Ramírez, J. Vía and I. Santamaría are with the Department of Communications Engineering, University of Cantabria, 39005 Santander, Spain (e-mail: {ramirezgd,jvia,nacho}@gtas.dicom.unican.es).

Gonzalo Vazquez-Vilar and Roberto López-Valcarce are with the Department of Signal Theory and Communications, University of Vigo, 36310 Vigo, Spain (e-mail: {gvazquez,valcarce}@gts.uvigo.es).

This work was presented in part at the 2nd IAPR International Workshop on Cognitive Information Processing (CIP 2010), Elba Island, Italy, June 2010 and at the 6th IEEE Sensor Array and Multichannel Signal Processing, Jerusalem, Israel, October 2010.

variances. This model is justified, for example, when tolerances in the components of the analog frontends at different antennas result in deviations of the noise level from antenna to antenna. The GLRT for this case requires solving a non-convex optimization problem. We propose an efficient numerical method based on an alternating minimization approach to compute the exact GLRT statistic. Additionally we show that this detector admits a closed-form expression in the asymptotic low SNR regime.

3) The proposed GLRT detectors are generalized to signals with unknown power spectral density (PSD), extending [17]–[19] to rank-P signals. This is of special interest in applications with frequency selective channels and/or temporally colored noise.

Our results are related to other works based on the GLRT framework. When the signal covariance matrix is unstructured, and the noise assumed iid, the GLRT is the well-known *test for sphericity* [20], which was applied to CR in [21], [22]. For $P = 1$ and iid noises the GLRT is derived in [6] and its application to CR was presented in [7], [9]. In [21], [22], the authors derived the GLRT for $P > 1$ under the assumption of iid noises with known variance. In [21] the unknown noise variance is handled heuristically, estimating this parameter as the smallest eigenvalue of the sample covariance matrix.

In [23] the GLRT was derived for the case of an unstructured signal covariance matrix for non-iid noises. This detector was later applied to array signal processing in [24], [25]. Other detectors which can handle different (unknown) noise variances have been proposed in [8], [26], [27]. However they either assume rank-1 primary signals or unstructured signals. A GLRT framework has also been applied in [28] assuming certain prior information of the unknown parameters, however the multiatenna setting is only marginally treated.

Notation: We use light-face letters for scalars, and boldface uppercase and lowercase letters for matrices and vectors, respectively. The elements of matrix $\mathbf{A}$ and vector $\mathbf{x}$ are denoted by $[\mathbf{A}]_{i,j}$ and x_i respectively. Calligraphic uppercase letters denote block-Toeplitz matrices. $\mathrm{diag}(\mathbf{x})$ is a diagonal matrix with the elements of vector $\mathbf{x}$ on its diagonal. Other notation is summarized in Table I.

$\hat{(\cdot)}$	Estimated matrices, vectors or scalars
$\det(\mathbf{A})$, $\mathrm{tr}(\mathbf{A})$	Determinant and trace of $\mathbf{A}$
$\mathrm{vec}\,(\mathbf{A})$	Column-wise vectorization of $\mathbf{A}$
$\mathbf{0}_L$	Zero $L \times 1$ vector or $L \times L$ matrix
$\mathbf{a}_k$	k-th column of matrix $\mathbf{A}$
$E[\cdot]$	Expectation operator
$\mathcal{F}(\cdot)$	Discrete-time Fourier transform
$\mathbf{x} \sim \mathcal{CN}(\boldsymbol{\mu}, \mathbf{R})$	Complex circular Gaussian random vector of mean $\boldsymbol{\mu}$ and covariance matrix $\mathbf{R}$
$\odot$	Hadamard product
$(h * s)\,[n]$	Convolution operation between $h[n]$ and $s[n]$
$\delta[m]$	Discrete delta impulse

TABLE I: Notation used in the paper.

II. Problem formulation

Consider a spectrum monitor equipped with L antennas which is to sense a given frequency channel. The received signals are downconverted and sampled at the Nyquist rate. No synchronization with any potentially present primary signal is assumed. Primary transmission, if present, is known to have spatial rank P, and a frequency-flat channel is assumed. Thus, for a single observation $\mathbf{x} \in \mathbb{C}^L$, the hypothesis testing problem can be written as

$$\begin{aligned} \mathcal{H}_1 &: \mathbf{x} = \mathbf{H}\mathbf{s} + \mathbf{v}, \\ \mathcal{H}_0 &: \mathbf{x} = \mathbf{v}, \end{aligned} \tag{1}$$

where $\mathbf{s} \in \mathbb{C}^P$ is the primary signal, $\mathbf{H} \in \mathbb{C}^{L \times P}$ is the unknown multiple-input multiple-output (MIMO) channel between the primary user and the spectrum sensor, and $\mathbf{v} \in \mathbb{C}^L$ is the additive noise, which is assumed to be zero-mean, spatially uncorrelated, circular complex Gaussian.

We model $\mathbf{s}$ as zero-mean circular complex Gaussian, which is particularly accurate if the primary transmitter uses orthogonal frequency division multiplexing (OFDM). Even if this is not the case, the Gaussian model leads to tractable analysis and useful detectors. It is assumed that $\mathbf{s}$ is spatially white and power-normalized, as any spatial correlation and scaling of the primary signal can be absorbed in the channel matrix $\mathbf{H}$. For the time being, we will assume that the primary signal and the noise are temporally white[1]. Taking this into account, the (spatial) covariance matrices of the primary signal and noise are given by

$$E\left[\mathbf{s}\mathbf{s}^H\right] = \mathbf{I}_P, \qquad E\left[\mathbf{v}\mathbf{v}^H\right] = \boldsymbol{\Sigma}^2, \tag{2}$$

where $\mathbf{I}_P$ is the identity matrix of size $P \times P$ and $\boldsymbol{\Sigma}^2$ is an unknown diagonal covariance matrix. The detection problem in (1) amounts to testing between two different structures for the covariance of the vector-valued random variable $\mathbf{x} \sim \mathcal{CN}\left(\mathbf{0}_L, \mathbf{R}\right)$:

$$\begin{aligned} \mathcal{H}_1 &: \mathbf{R} = \mathbf{H}\mathbf{H}^H + \boldsymbol{\Sigma}^2, \\ \mathcal{H}_0 &: \mathbf{R} = \boldsymbol{\Sigma}^2. \end{aligned} \tag{3}$$

That is, under $\mathcal{H}_0$ the covariance matrix $\mathbf{R}$ is diagonal whereas under $\mathcal{H}_1$ it is a rank-P matrix plus a diagonal one. We shall assume that $\mathbf{H}$ has full rank.

III. Derivation of the GLRT for iid noises

As a first step, we derive a detector for the simpler case of iid noises, i.e., $\boldsymbol{\Sigma}^2 = \sigma^2\mathbf{I}$, which amounts to saying that all the L analog frontends are perfectly calibrated. As there are unknown parameters under both hypotheses, the Neyman-Pearson detector is not implementable for this composite test. Therefore, we adopt a GLRT approach, since it usually results in simple detectors with good performance [29].

We shall consider $M \geq L$ snapshots $\mathbf{x}_0, \ldots, \mathbf{x}_{M-1}$. Assuming that the channel remains constant during the sensing

[1]These results will be extended in Section V to the case in which noise and primary signals are time series with *unknown* temporal structure.

period, these can be regarded as iid realizations of $\mathbf{x} \sim \mathcal{CN}(\mathbf{0}_L, \mathbf{R})$. The likelihood is given by the product of the individual pdfs, i.e.,

$$p\left(\mathbf{x}_0, \ldots, \mathbf{x}_{M-1}; \mathbf{R}\right) = \frac{1}{\pi^{LM} \det\left(\mathbf{R}\right)^M} \exp\left\{-M \mathrm{tr}\left(\hat{\mathbf{R}}\mathbf{R}^{-1}\right)\right\}, \quad (4)$$

where $\hat{\mathbf{R}} = \frac{1}{M}\sum_{m=0}^{M-1} \mathbf{x}_m \mathbf{x}_m^H$ is the sample covariance matrix. The GLRT for $\mathcal{H}_0 : \mathbf{R} = \sigma^2\mathbf{I}$ vs. $\mathcal{H}_1 : \mathbf{R} = \mathbf{H}\mathbf{H}^H + \sigma^2\mathbf{I}$ is based on the generalized likelihood ratio $\mathscr{L}$ [29]

$$\mathscr{L} = \frac{\max\limits_{\sigma^2} p\left(\mathbf{x}_0, \ldots, \mathbf{x}_{M-1}; \sigma^2\right)}{\max\limits_{\mathbf{H}, \sigma^2} p\left(\mathbf{x}_0, \ldots, \mathbf{x}_{M-1}; \mathbf{H}, \sigma^2\right)} \underset{\mathcal{H}_1}{\overset{\mathcal{H}_0}{\gtrless}} \eta, \quad (5)$$

with η a threshold. First, the maximum likelihood (ML) estimate of the noise variance under $\mathcal{H}_0$ is given by

$$\hat{\sigma}^2 = \frac{1}{L}\mathrm{tr}\left(\hat{\mathbf{R}}\right). \quad (6)$$

In order to obtain the ML estimates under $\mathcal{H}_1$, we consider two cases depending on the rank P.

Lemma 1: If $P \geq L-1$, the ML estimates of $\mathbf{H}$ and σ^2 satisfy $\hat{\mathbf{H}}\hat{\mathbf{H}}^H + \hat{\sigma}^2\mathbf{I} = \hat{\mathbf{R}}$.

Proof: For $P \geq L-1$, $\mathbf{R} = \mathbf{H}\mathbf{H}^H + \sigma^2\mathbf{I}$ has no additional structure besides being positive definite Hermitian. In that case, the log-likelihood is maximized for $\mathbf{R} = \hat{\mathbf{R}}$, as shown in [30]. ∎

Thus, for $P \geq L-1$, the GLRT is the well-known *Sphericity test* [20]

$$\log \mathscr{L} = ML \log\left[\frac{\det^{1/L}\left(\hat{\mathbf{R}}\right)}{\frac{1}{L}\mathrm{trace}\left(\hat{\mathbf{R}}\right)}\right]. \quad (7)$$

When $P < L-1$, the low-rank structure of the primary signal can be used to further improve the detection. In that case, to obtain the ML estimates under $\mathcal{H}_1$, let $\mathbf{H}\mathbf{H}^H = \mathbf{U}\mathbf{\Psi}^2\mathbf{U}^H$ be the eigenvalue decomposition (EVD) of $\mathbf{H}\mathbf{H}^H$, with

$$\mathbf{\Psi}^2 = \mathrm{diag}(\psi_1^2, \psi_2^2, \ldots, \psi_P^2, 0, 0, \ldots, 0), \quad (8)$$

and $\psi_1 \geq \psi_2 \geq \cdots \geq \psi_P$.

Lemma 2: Let $\hat{\mathbf{R}} = \mathbf{W}\mathrm{diag}\left(\lambda_1, \ldots, \lambda_L\right)\mathbf{W}^H$ be the EVD of the sample covariance matrix, with $\lambda_1 \geq \lambda_2 \geq \cdots \geq \lambda_L$. For $P < L-1$, the ML estimates of $\mathbf{U}$, $\mathbf{\Psi}^2$ and σ^2 under $\mathcal{H}_1$ are given by

$$\hat{\mathbf{U}} = \mathbf{W}, \qquad \hat{\sigma}^2 = \frac{1}{L-P}\sum_{k=P+1}^{L} \lambda_k, \quad (9)$$

$$\hat{\psi}_i^2 = \lambda_i - \hat{\sigma}^2, \quad i = 1, \ldots, P. \quad (10)$$

Proof: This result was proved by Anderson in [31]. ∎

Taking into account (6) and Lemma 2, the log-GLRT for $P < L-1$ is given, after some straightforward manipulations, by

$$\log \mathscr{L} = ML \log\left[\frac{\left(\prod_{i=1}^{L}\lambda_i\right)^{1/L}}{\frac{1}{L}\sum_{i=1}^{L}\lambda_i}\right] - M\left(L-P\right)\log\left[\frac{\left(\prod_{i=P+1}^{L}\lambda_i\right)^{1/(L-P)}}{\frac{1}{L-P}\sum_{i=P+1}^{L}\lambda_i}\right] \underset{\mathcal{H}_1}{\overset{\mathcal{H}_0}{\gtrless}} \eta, \quad (11)$$

Note that the logarithmic terms in (11) are functions of the ratio between the geometric and arithmetic means of all eigenvalues and the $L-P$ smallest eigenvalues of $\hat{\mathbf{R}}$, respectively. The first term is the statistic of the sphericity test (7), whereas the second term can be seen as a test for the sphericity of the noise subspace, or as a *reference* for sphericity due to finite sample size effects (since as $M \to \infty$, then $\hat{\mathbf{R}} \to \mathbf{R}$ and thus $\lambda_i \to \sigma^2$ for $i = P+1, \ldots, L$, so that the second term in (11) goes to zero). Thus, the log-GLRT may be seen as a *sphericity ratio* (quotient between the sphericity statistics of the sample covariance matrix and its noise subspace).

Remark 1: The GLRT in (11) generalizes the results in [6], [7], [9] obtained for the special case of $P = 1$.

IV. Derivation of the GLRT for non-iid noises

In this section we derive the GLRT for the more involved model of non-iid noises. In this case, the only constraint on $\mathbf{\Sigma}^2$ is being diagonal with positive entries. Let us start by the ML estimate of $\mathbf{\Sigma}^2$ under $\mathcal{H}_0$, which is given by [24], [25]

$$\hat{\mathbf{\Sigma}}^2 = \mathrm{diag}\left([\hat{\mathbf{R}}]_{1,1}, \ldots, [\hat{\mathbf{R}}]_{L,L}\right) = \hat{\mathbf{D}}. \quad (12)$$

Similar to the case of iid noises, we study first the effect of the signal rank P on the ML estimate of the covariance matrix.

Lemma 3: If $P \geq L - \sqrt{L}$, the ML estimates of $\mathbf{H}$ and $\mathbf{\Sigma}^2$ under $\mathcal{H}_1$ satisfy $\hat{\mathbf{H}}\hat{\mathbf{H}}^H + \hat{\mathbf{\Sigma}}^2 = \hat{\mathbf{R}}$.

Proof: The proof can be found in [18], [24]. It hinges on the fact that if $P \geq L - \sqrt{L}$, then $\mathbf{H}\mathbf{H}^H + \mathbf{\Sigma}^2$ has no further structure beyond being positive definite Hermitian. ∎

Hence, for $P \geq L - \sqrt{L}$, the GLRT is given by the *Hadamard ratio* of the sample covariance matrix [23]–[25]:

$$\mathscr{L} = \frac{\det\left(\hat{\mathbf{R}}\right)}{\prod_{i=1}^{L}[\hat{\mathbf{R}}]_{i,i}}. \quad (13)$$

If $P < L - \sqrt{L}$, the low-rank structure of the primary signal can be further exploited. In order to simplify the derivation of the ML estimates under $\mathcal{H}_1$, let $\hat{\mathbf{R}}_{\mathbf{\Sigma}} = \mathbf{\Sigma}^{-1}\hat{\mathbf{R}}\mathbf{\Sigma}^{-1}$ (the *whitened* sample covariance matrix) and $\mathbf{H}_{\mathbf{\Sigma}} = \mathbf{\Sigma}^{-1}\mathbf{H}$. We can rewrite the log-likelihood as

$$\log p\left(\mathbf{x}_0, \ldots, \mathbf{x}_{M-1}; \mathbf{H}_{\mathbf{\Sigma}}, \mathbf{\Sigma}^2\right) = -LM\log\pi - M\log\det\left(\mathbf{H}_{\mathbf{\Sigma}}\mathbf{H}_{\mathbf{\Sigma}}^H + \mathbf{I}\right) - M\log\det\left(\mathbf{\Sigma}^2\right) - M\mathrm{tr}\left[\hat{\mathbf{R}}_{\mathbf{\Sigma}}\left(\mathbf{H}_{\mathbf{\Sigma}}\mathbf{H}_{\mathbf{\Sigma}}^H + \mathbf{I}\right)^{-1}\right]. \quad (14)$$

Let $\mathbf{H}_{\mathbf{\Sigma}}\mathbf{H}_{\mathbf{\Sigma}}^H = \mathbf{G}\mathbf{\Phi}^2\mathbf{G}^H$ be the EVD of $\mathbf{H}_{\mathbf{\Sigma}}\mathbf{H}_{\mathbf{\Sigma}}^H$. The ML estimates of $\mathbf{G}$ and $\mathbf{\Phi}^2$ are given next.

Lemma 4: Let $\hat{\mathbf{R}}_{\boldsymbol{\Sigma}} = \mathbf{Q}\text{diag}\left(\gamma_1, \ldots, \gamma_L\right)\mathbf{Q}^H$ be the EVD of $\hat{\mathbf{R}}_{\boldsymbol{\Sigma}}$, with $\gamma_1 \geq \cdots \geq \gamma_L$. The ML estimates of $\mathbf{G}$ and $\boldsymbol{\Phi}^2 = \text{diag}\left(\phi_1, \ldots, \phi_L\right)$ (which are functions of $\boldsymbol{\Sigma}^2$) are

$$\hat{\mathbf{G}} = \mathbf{Q}, \tag{15}$$

$$\hat{\phi}_i^2 = \begin{cases} \gamma_i - 1, & i = 1, \ldots, P, \\ 0, & i = P+1, \ldots, L. \end{cases} \tag{16}$$

Proof: Once $\hat{\mathbf{R}}$ and $\mathbf{H}$ have been prewhitened, the problem reduces to the iid case and, therefore, the proof follows the same lines as those in [31]. ∎

Finally, replacing the ML estimate of $\mathbf{H}_{\boldsymbol{\Sigma}}\mathbf{H}_{\boldsymbol{\Sigma}}^H$ into (14) we obtain

$$\log p\left(\mathbf{x}_0, \ldots, \mathbf{x}_{M-1}; \boldsymbol{\Sigma}^2\right) = -LM\log\pi - MP - M\log\det\left(\hat{\mathbf{R}}\right) - M\sum_{i=P+1}^{L}\left[\gamma_i - \log\gamma_i\right]. \tag{17}$$

As previously mentioned, for unstructured covariance matrices, i.e. $P \geq L - \sqrt{L}$, there does exist a closed-form GLRT given by (13). However, to the best of our knowledge, the maximization of (17) with respect to $\boldsymbol{\Sigma}^2$ does not admit a closed-form solution if $P < L - \sqrt{L}$. We present two different approaches: an alternating optimization scheme and a closed-form GLRT detector obtained in the limit of asymptotically small SNR.

A. Alternating optimization

The ML estimation problem in (14) can be written as

$$\begin{aligned} \underset{\mathbf{H}_{\boldsymbol{\Sigma}}, \boldsymbol{\Sigma}}{\text{minimize}} \;& \text{tr}\left(\hat{\mathbf{R}}\boldsymbol{\Sigma}^{-1}\mathbf{R}_{\boldsymbol{\Sigma}}^{-1}\boldsymbol{\Sigma}^{-1}\right) \\ & - \log\det\left(\boldsymbol{\Sigma}^{-2}\right) + \log\det\mathbf{R}_{\boldsymbol{\Sigma}}, \\ \text{subject to} \;& \mathbf{R}_{\boldsymbol{\Sigma}} = \mathbf{I}_L + \mathbf{H}_{\boldsymbol{\Sigma}}\mathbf{H}_{\boldsymbol{\Sigma}}^H, \\ & [\boldsymbol{\Sigma}]_{i,i} \geq 0. \end{aligned} \tag{18}$$

While this optimization problem is non-convex, it is possible to partition the free variables in two different sets to obtain an alternating optimization scheme. Then, we will alternatively perform the minimization over each set of parameters while the remaining ones are held fixed. Since at each step the value of the cost function can only decrease the method is guaranteed to converge to a (local) minimum.

From (18), we note that the individual minimization with respect to $\boldsymbol{\Sigma}$ (considering $\mathbf{H}_{\boldsymbol{\Sigma}}$ fixed) and with respect to $\mathbf{H}_{\boldsymbol{\Sigma}}$ (considering $\boldsymbol{\Sigma}$ fixed) can be easily written as convex problems individually, and, therefore, they can be efficiently solved.

Minimization with respect to $\mathbf{H}_{\boldsymbol{\Sigma}}$. For fixed $\boldsymbol{\Sigma}$, the optimal $\mathbf{H}_{\boldsymbol{\Sigma}}$ minimizing (18) is (up to a right multiplication by a unitary matrix) given by Lemma 4, that is

$$\hat{\mathbf{H}}_{\boldsymbol{\Sigma}} = \begin{bmatrix}\mathbf{q}_1 & \cdots & \mathbf{q}_P\end{bmatrix}\left(\text{diag}\left(\gamma_1, \ldots, \gamma_P\right) - \mathbf{I}_P\right)^{1/2}. \tag{19}$$

Minimization with respect to $\boldsymbol{\Sigma}$. For fixed $\mathbf{H}_{\boldsymbol{\Sigma}}$ the minimization problem in (18) reduces to

$$\begin{aligned} \underset{\boldsymbol{\Sigma}}{\text{minimize}} \;& \text{tr}\left(\hat{\mathbf{R}}\boldsymbol{\Sigma}^{-1}\mathbf{R}_{\boldsymbol{\Sigma}}^{-1}\boldsymbol{\Sigma}^{-1}\right) - \log\det\left(\boldsymbol{\Sigma}^{-2}\right) \\ \text{subject to} \;& [\boldsymbol{\Sigma}]_{i,i} \geq 0. \end{aligned} \tag{20}$$

Algorithm 1: Iterative estimation of $\mathbf{H}_{\boldsymbol{\Sigma}}$ and $\boldsymbol{\Sigma}$ via alternating optimization.

Input: Starting point $\boldsymbol{\alpha}_{(0)}$ and $\hat{\mathbf{R}}$.
Output: ML estimates of $\mathbf{H}_{\boldsymbol{\Sigma}}$ and $\boldsymbol{\Sigma}$.
Initialize: $n = 0$
repeat
- Compute $\boldsymbol{\Sigma}_{(n)}^{-1} = \text{diag}(\boldsymbol{\alpha}_n)$
- Obtain $\hat{\mathbf{R}}_{\boldsymbol{\Sigma}}^{(n+1)} = \boldsymbol{\Sigma}_{(n)}^{-1}\hat{\mathbf{R}}\boldsymbol{\Sigma}_{(n)}^{-1}$ and its EVD
- Compute $\mathbf{H}_{\boldsymbol{\Sigma}}^{(n+1)}$ from (19) (fixed $\boldsymbol{\Sigma}_{(n)}^{-1}$)
- Solve (21) to obtain $\boldsymbol{\alpha}_{(n+1)}$ (fixed $\mathbf{H}_{\boldsymbol{\Sigma}}^{(n+1)}$)
- Update $n = n + 1$

until Convergence

Defining the vector $\boldsymbol{\alpha} = \left[[\boldsymbol{\Sigma}^{-1}]_{1,1}, \ldots, [\boldsymbol{\Sigma}^{-1}]_{L,L}\right]^T$, the trace term in (20) can be reorganized to obtain an equivalent minimization problem given by

$$\begin{aligned} \underset{\boldsymbol{\alpha}}{\text{minimize}} \;& \boldsymbol{\alpha}^T(\hat{\mathbf{R}}^T \odot \mathbf{R}_{\boldsymbol{\Sigma}}^{-1})\boldsymbol{\alpha} - \sum_{i=1}^{L}\log\alpha_i^2 \\ \text{subject to} \;& \alpha_i \geq 0. \end{aligned} \tag{21}$$

Note that, given the trace term in (20), the matrix $\hat{\mathbf{R}}^T \odot \mathbf{R}_{\boldsymbol{\Sigma}}^{-1}$ is positive semidefinite. Hence, the problem (21) is convex with respect to the parameter vector $\boldsymbol{\alpha}$ and, therefore, it can be efficiently solved using any convex optimization solver.

The proposed alternating minimization algorithm is summarized in Alg. 1. While the alternating minimization approach does not guarantee that the global maximizer of the log-likelihood is found, in the numerical experiments conducted this detector shows good performance.

B. Low SNR approximation of the GLRT

The usefulness of the detector given in Alg. 1 in practical settings may be hindered by its complexity. In this context, simpler closed-form detectors become of practical interest. Now, we derive a closed-form expression for the GLRT in the low SNR regime, of particular interest in CR applications. As the SNR goes to zero, the covariance matrix will become close to diagonal, and thus it is possible to approximate the ML estimate of $\boldsymbol{\Sigma}^2$ as $\hat{\boldsymbol{\Sigma}}^2 \approx \hat{\mathbf{D}}$, where $\hat{\mathbf{D}}$ is defined in (12). Substituting this back into (17), we obtain the final compressed log-likelihood:

$$\log p\left(\mathbf{x}_0, \ldots, \mathbf{x}_{M-1}\right) = -LM\log\pi - MP - M\log\det\left(\hat{\mathbf{R}}\right) - M\sum_{i=P+1}^{L}\left[\beta_i - \log\beta_i\right]. \tag{22}$$

where β_i is the i-th largest eigenvalue of the sample spatial coherence matrix $\hat{\mathbf{C}} = \hat{\mathbf{D}}^{-1/2}\hat{\mathbf{R}}\hat{\mathbf{D}}^{-1/2}$. Then, the asymptotic log-GLRT is

$$\log\mathscr{L} \approx M\sum_{i=1}^{P}\left[\log\beta_i - \beta_i\right] + MP \underset{\mathcal{H}_1}{\overset{\mathcal{H}_0}{\gtrless}} \eta. \tag{23}$$

Alternatively, (23) can be rewriten as

$$\log \mathscr{L} \approx MP + M \log \prod_{i=1}^{P} \beta_i e^{-\beta_i} \underset{\mathcal{H}_1}{\overset{\mathcal{H}_0}{\gtrless}} \eta, \tag{24}$$

and, thus, the test statistic is seen to be given by the product of the P largest eigenvalues of $\hat{\mathbf{C}}$, each equalized by an exponential term. Note that $\beta e^{-\beta}$ is maximum at $\beta = 1$. Hence, the statistic $\prod_{i=1}^{P} \beta_i e^{-\beta_i}$ measures, in some sense, how far the vector of the P largest eigenvalues $[\beta_1 \cdots \beta_P]$ is from the vector of all ones. Note that (23) yields a closed-form test, in contrast with the iterative scheme presented in the previous section.

V. Extension to time series with temporal structure

We extend now the detectors in Sections III and IV in order to deal with frequency-selective channels, as well as *unknown* temporal correlation in signals and noise.

A. Problem formulation

The detection problem can be expressed now as

$$\begin{array}{ll} \mathcal{H}_1 : \mathbf{x}[n] = (\mathbf{H} * \mathbf{s})[n] + \mathbf{v}[n], & n = 0, \ldots, N-1, \\ \mathcal{H}_0 : \mathbf{x}[n] = \mathbf{v}[n], & n = 0, \ldots, N-1, \end{array} \tag{25}$$

where $\mathbf{s}[n] \in \mathbb{C}^P$ is the wide sense stationary (WSS) zero-mean circular complex Gaussian primary signal; $\mathbf{H}[n] \in \mathbb{C}^{L \times P}$ is the frequency-selective MIMO channel between the primary user and the spectrum monitor; and $\mathbf{v}[n] \in \mathbb{C}^L$ is the additive noise vector, which is assumed to be WSS zero-mean circular complex Gaussian and spatially uncorrelated, i.e., $E\left[v_i[n] v_k^*[m]\right] = 0$ for $i \neq k$ and $\forall n, m$. No assumptions are made about the *temporal* correlation of the primary signal or the noise processes. Note, however, that any spatial and temporal correlation present in the signal can be absorbed in the unknown channel without altering the model. Therefore, the matrix-valued covariance function of the primary signal and the noise are given by

$$E\left[\mathbf{s}[n]\mathbf{s}^H[n-m]\right] = \mathbf{I}\delta[m], \tag{26}$$

$$E\left[\mathbf{v}[n]\mathbf{v}^H[n-m]\right] = \mathbf{\Sigma}^2[m], \tag{27}$$

where $\mathbf{\Sigma}^2[m]$ is a diagonal matrix for all values of m.

Let us introduce the data matrix

$$\mathbf{X} = \begin{bmatrix} \mathbf{x}[0] & \mathbf{x}[1] & \ldots & \mathbf{x}[N-1] \end{bmatrix} \in \mathbb{C}^{L \times N}, \tag{28}$$

where the i-th row contains N samples of the time series $\{x_i[n]\}$ at the i-th antenna, and the n-th column is the n-th sample of the vector-valued time series. The vector $\mathbf{z} = \mathrm{vec}(\mathbf{X})$ stacks the columns of $\mathbf{X}$, and in view of the WSS assumption, its block-Toeplitz covariance matrix $\mathcal{R} \in \mathbb{C}^{LN \times LN}$ is given by

$$\mathcal{R} = \begin{bmatrix} \mathbf{R}[0] & \mathbf{R}[-1] & \cdots & \mathbf{R}[-N+1] \\ \mathbf{R}[1] & \mathbf{R}[0] & \cdots & \mathbf{R}[-N+2] \\ \vdots & \vdots & \ddots & \vdots \\ \mathbf{R}[N-1] & \mathbf{R}[N-2] & \cdots & \mathbf{R}[0] \end{bmatrix}, \tag{29}$$

where $\mathbf{R}[m] = E\left[\mathbf{x}[n]\mathbf{x}^H[n-m]\right]$ is a matrix-valued covariance function. Therefore, under the Gaussian assumption, the hypothesis testing problem becomes

$$\begin{aligned} \mathcal{H}_1 &: \mathbf{z} \sim \mathcal{CN}(\mathbf{0}_{LN}, \mathcal{R}_1), \\ \mathcal{H}_0 &: \mathbf{z} \sim \mathcal{CN}(\mathbf{0}_{LN}, \mathcal{R}_0). \end{aligned}$$

We are testing two different block-Toeplitz matrices where each block has a different structure under each hypothesis. Under $\mathcal{H}_0$ each block $\mathbf{R}[m] = \mathbf{\Sigma}^2[m]$ is diagonal, whereas, under $\mathcal{H}_1$, it is given by

$$\mathbf{R}[m] = \sum_k \mathbf{H}[k]\mathbf{H}^H[k-m] + \mathbf{\Sigma}^2[m]. \tag{30}$$

B. Asymptotic log-likelihood

The structure of $\mathcal{R}_1$ induced by the rank-P primary signal, along with the block-Toeplitz structure, prevents the ML estimation of $\mathcal{R}_1$ in closed-form, even in the case of iid noises. In fact, the ML estimation of Toeplitz covariance matrices is known to be a non-convex problem with no closed-form solution [32]. To overcome this limitation, we introduce Theorem 1, which states the convergence (in the mean square sense) between the log-likelihood and its asymptotic version. This theorem allows us to work with the log-likelihood in the frequency domain which, as we will see, simplifies the derivation of the GLRT (actually, the asymptotic GLRT). The asymptotic log-likelihood is now a function of the estimated and theoretical power spectral density (PSD) matrices instead of being a function of the estimated and theoretical covariance matrices. Additionally, the proposed asymptotic log-likelihood is an extension of Whittle's likelihood [33], [34] to multivariate Gaussian processes.

Let us introduce some definitions before presenting the theorem. Consider an experiment producing M ($M \geq L$) independent realizations[2] of the data vector $\mathbf{z}$. Then, its log-likelihood is given by

$$\begin{aligned} \log p(\mathbf{z}_0, \ldots, \mathbf{z}_{M-1}; \mathcal{R}) = &- LNM \log \pi - M \log \det(\mathcal{R}) \\ &- M \mathrm{tr}\left(\hat{\mathbf{R}}\mathcal{R}^{-1}\right), \end{aligned} \tag{31}$$

and the asymptotic ($N \to \infty$) log-likelihood is

$$\begin{aligned} \log p\left(\mathbf{z}_0, \ldots, \mathbf{z}_{M-1}; \mathbf{S}\left(e^{j\theta}\right)\right) = &-LNM \log \pi \\ &- NM \int_{-\pi}^{\pi} \log \det\left(\mathbf{S}\left(e^{j\theta}\right)\right) \frac{d\theta}{2\pi} \\ &- NM \int_{-\pi}^{\pi} \mathrm{tr}\left(\hat{\mathbf{S}}\left(e^{j\theta}\right)\mathbf{S}^{-1}\left(e^{j\theta}\right)\right) \frac{d\theta}{2\pi}, \end{aligned} \tag{32}$$

where $\mathcal{R}$ is the theoretical block-Toeplitz covariance matrix, $\mathbf{S}\left(e^{j\theta}\right) = \mathcal{F}(\mathbf{R}[m])$ is the theoretical PSD matrix, and their sample estimates are $\hat{\mathbf{R}} = \frac{1}{M}\sum_{i=0}^{M-1} \mathbf{z}_i \mathbf{z}_i^H$ and $\hat{\mathbf{S}}\left(e^{j\theta}\right) = \frac{1}{M}\sum_{i=0}^{M-1} \mathbf{x}_i\left(e^{j\theta}\right)\mathbf{x}_i^H\left(e^{j\theta}\right)$, with $\mathbf{x}_i\left(e^{j\theta}\right) = \frac{1}{\sqrt{N}}\sum_{n=0}^{N-1} \mathbf{x}_i[n] e^{-j\theta n}$.

[2] In this case, the *snapshots* are matrix-valued.

Theorem 1: As $N \to \infty$, the asymptotic log-likelihood converges in the mean square sense to the true log-likelihood:

$$\lim_{N\to\infty} E\left[\left|\frac{1}{N}\left[\log p\left(\mathbf{z}_0,\ldots,\mathbf{z}_{M-1};\mathcal{R}\right)\right.\right.\right.$$
$$\left.\left.\left.-\log p\left(\mathbf{z}_0,\ldots,\mathbf{z}_{M-1};\mathbf{S}\left(e^{j\theta}\right)\right)\right]\right|^2\right]=0. \quad (33)$$

Proof: The proof can be found in Appendix A. ∎

As a direct consequence of Theorem 1, the hypothesis test asymptotically becomes

$$\mathcal{H}_1 : \mathbf{x}\left(e^{j\theta}\right) \sim \mathcal{CN}\left(\mathbf{0}, \mathbf{S}_1\left(e^{j\theta}\right)\right), \quad (34)$$
$$\mathcal{H}_0 : \mathbf{x}\left(e^{j\theta}\right) \sim \mathcal{CN}\left(\mathbf{0}, \mathbf{S}_0\left(e^{j\theta}\right)\right), \quad (35)$$

where $\mathbf{S}_1\left(e^{j\theta}\right) = \mathbf{H}\left(e^{j\theta}\right)\mathbf{H}^H\left(e^{j\theta}\right) + \mathbf{\Sigma}^2\left(e^{j\theta}\right)$, $\mathbf{S}_0\left(e^{j\theta}\right) = \mathbf{\Sigma}^2\left(e^{j\theta}\right)$, $\mathbf{H}\left(e^{j\theta}\right)$ is the Fourier transform of the MIMO channel and $\mathbf{\Sigma}^2\left(e^{j\theta}\right)$ is a diagonal matrix which contains the PSD of the noises. Therefore, under $\mathcal{H}_0$ the PSD matrix is diagonal, whereas under $\mathcal{H}_1$ it is the sum of a rank-P matrix plus a diagonal one.

C. Derivation of the GLRT

Without imposing any temporal structure to the time series, the ML estimation of the unknown parameters can be carried out on a frequency-by-frequency basis. Thus, we can directly apply the results from Sections III and IV. First, the log-GLRT for the case of noises with equal PSDs, i.e., $\mathbf{\Sigma}^2(e^{j\theta}) = S_v(e^{j\theta})\mathbf{I}$ and assuming $P < L-1$, is given by

$$\log\mathscr{L} = NML\int_{-\pi}^{\pi}\log\left[\frac{\left(\prod_{i=1}^{L}\lambda_i\left(e^{j\theta}\right)\right)^{1/L}}{\frac{1}{L}\sum_{i=1}^{L}\lambda_i\left(e^{j\theta}\right)}\right]\frac{d\theta}{2\pi}$$
$$-NM(L-P)\int_{-\pi}^{\pi}\log\left[\frac{\left(\prod_{i=P+1}^{L}\lambda_i\left(e^{j\theta}\right)\right)^{1/(L-P)}}{\frac{1}{L-P}\sum_{i=P+1}^{L}\lambda_i\left(e^{j\theta}\right)}\right]\frac{d\theta}{2\pi}, \quad (36)$$

where $\lambda_i\left(e^{j\theta}\right)$ is the i-th largest eigenvalue of $\hat{\mathbf{S}}\left(e^{j\theta}\right)$. The asymptotic log-GLRT for time series with unknown temporal structure is the integral of the frequency-wise GLRT statistic for white vector-valued time-series, derived in (11).

For the case of noises with different PSDs along the antennas, and assuming $P < L - \sqrt{L}$, the log-GLRT in the low SNR region[3] is approximately given by

$$\log\mathscr{L} \approx NM\int_{-\pi}^{\pi}\sum_{i=1}^{P}\log\beta_i\left(e^{j\theta}\right)\frac{d\theta}{2\pi}$$
$$-NM\int_{-\pi}^{\pi}\sum_{i=1}^{P}\beta_i\left(e^{j\theta}\right)\frac{d\theta}{2\pi}+NMP, \quad (37)$$

where β_i is the i-th largest eigenvalue of the coherence matrix

$$\hat{\mathbf{C}}\left(e^{j\theta}\right) = \hat{\mathbf{D}}^{-1/2}\left(e^{j\theta}\right)\hat{\mathbf{S}}\left(e^{j\theta}\right)\hat{\mathbf{D}}^{-1/2}\left(e^{j\theta}\right) \quad (38)$$

[3]For other SNR regimes, it would be possible to apply, on a frequency-by-frequency basis, the alternating minimization algorithm presented in Section IV-A.

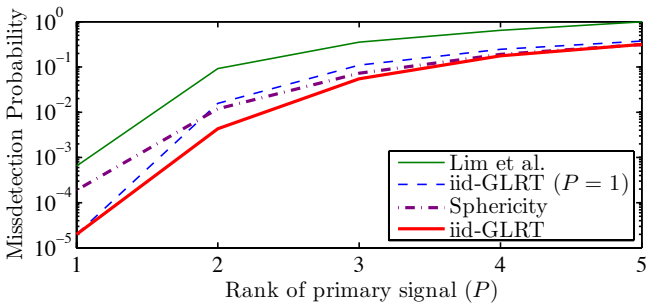

(a) iid noise

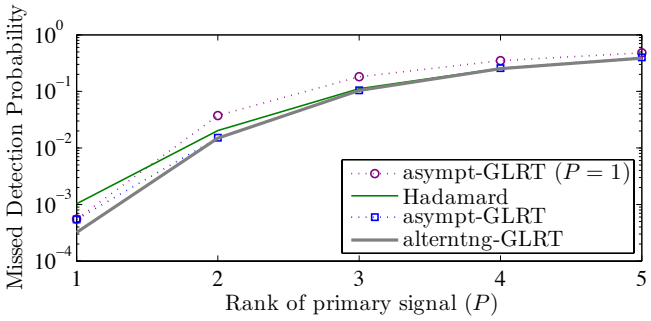

(b) non-iid noise

Fig. 1: Missed detection probability versus P.

and

$$\hat{\mathbf{D}}\left(e^{j\theta}\right) = \mathrm{diag}\left([\hat{\mathbf{S}}\left(e^{j\theta}\right)]_{1,1},\ldots,[\hat{\mathbf{S}}\left(e^{j\theta}\right)]_{L,L}\right). \quad (39)$$

The asymptotic log-GLRT is, again, the integral of the GLRT for vector-valued random variables.

VI. Numerical results

In this section we evaluate the performance of the proposed algorithms under different scenarios by means of Monte Carlo simulations. First, we consider frequency-flat channels and temporally white signals and noises. Unless otherwise specified, the noise level at each antenna is fixed for each experiment, and for each Monte Carlo realization the entries of the channel matrix $\mathbf{H}$ are independently drawn from a Gaussian distribution (thus obtaining a Rayleigh fading scenario) and scaled so that the SNR is constant during the experiment:

$$\text{SNR (dB)} = 10\log_{10}\frac{\mathrm{tr}(\mathbf{H}\mathbf{H}^H)}{\mathrm{tr}(\mathbf{\Sigma}^2)}. \quad (40)$$

We evaluate two detectors derived under the iid noise assumption: the proposed GLRT statistic in (11) denoted here by *iid-GLRT*, and the sphericity test or GLRT for non-structured primary signals [20] (denoted as *Sphericity*). In addition, three detectors derived for uncalibrated receivers ($\mathbf{\Sigma}^2$ diagonal with positive entries) are also evaluated: the proposed alternating optimization scheme from Algorithm 1 denoted here as *alterntng-GLRT*[4], the asymptotic closed-form

[4]Given the observed convergence properties, the iterations are stopped when the cost improvement between iterations is less than 10^{-5} with a maximum of 100 allowed iterations. As starting point we use an estimate given by the scaled low SNR asymptotic solution $\boldsymbol{\alpha}_0 = \sqrt{L/(L-P)}\left[[\hat{\mathbf{D}}]_{1,1}^{-1},\ldots,[\hat{\mathbf{D}}]_{L,L}^{-1}\right]^T$.

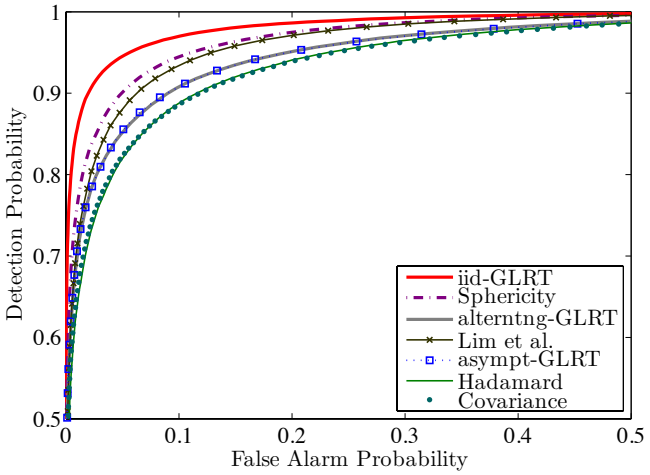

Fig. 2: ROC curve for the different detectors (SNR= -8 dB, $L = 4$ antennas, $M = 128$ samples) without noise power mismatch (noise level at each antenna equal to 0 dB). Signal rank $P = 1$.

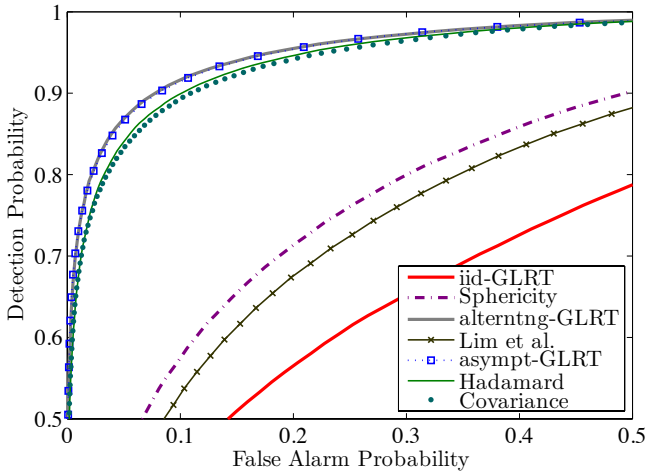

Fig. 3: ROC curve for the different detectors (SNR= -8 dB, $L = 4$ antennas, $M = 128$ samples) with noise power mismatch (noise powers at each antenna equal to 0, -1, 1.5 and -0.5 dB respectively). Signal rank $P = 1$.

detector in (23) (*asympt-GLRT*), the Hadamard ratio test [23] or GLRT for unstructured primary signals (13) (*Hadamard*). Additionally, we also include two heuristic detectors for comparison: the detector based on statistical covariances [27, Alg. 1] (*Covariance*) and that of Eqn. (32) in [21] (*Lim et al.*).

A. Detection performance for rank-P primary signals

First we compare the performance of the different schemes in terms of the spatial rank of the signal. Figure 1 shows the missed detection probability (for $P_{FA} = 0.01$) in a scenario with SNR $= -6$ dB, $L = 6$ antennas for primary signals with rank $P = 1, \ldots, 5$, for iid and non-iid noises. The number of samples is $M = 64$. Note that, for increasing P the structure present in the covariance matrix decreases. This effect translates into the performance degradation for all the detectors under study.

From Figs. 1a and 1b we can see that both for iid and non-iid noises the proposed GLRT detectors are the best performing detectors for arbitrary values of P. While the GLRTs for $P = 1$ present poor performance if the actual rank of the signal is larger than one, Sphericity and Hadamard ratio tests (which do not assume any structure on the primary signal) degrade for strong structure, i.e. small P. It is interesting to note however that as the rank of the signal grows (for $P \geq 4$) the Sphericity and Hadamard ratio tests offer similar performance to that of the rank-based detectors at a lower computational cost. Regarding the heuristic detectors, the covariance based detector (*Covariance*) presents virtually the same performance as the Hadamard ratio test and it was not included in the plot for clarity. On the other hand, the poor performance of the detector of *Lim et al.* [21] for all values of P is likely rooted in the heuristic estimation of the noise variance.

Finally, it is interesting to note that for $P > 1$, the advantage of the iterative scheme *alterntng-GLRT* over the asymptotic GLRT decreases. This can be explained from the fact that, as the total SNR is divided among a growing number of dimensions, the effective SNR per dimension decreases and one gets closer to the asymptotic regime for which *asympt-GLRT* was derived.

B. Noise mismatch effect on the detection performance

We now investigate the effect of a noise level mismatch at the different antennas on the different detectors. In order to focus on this effect we fix $P = 1$. Fig. 2 shows the corresponding receiver operating characteristic (ROC) curves in a scenario with iid noises. Note that the *iid-GLRT* test, corresponding to the GLRT under this model (rank-1 signals and iid noises), yields the best detection performance, whereas the detectors designed for non-uniform noise variances suffer a noticeable penalty. From the detectors designed for uncalibrated receivers, it is seen that the GLRT based schemes, both asymptotic and iterative, behave similarly and outperform the Hadamard ratio detector. The heuristic detector based on statistical covariances [27] presents almost the same performance as the Hadamard ratio test, while the detector of *Lim et al.* suffers a penalty compared to the GLRT for the same model.

Fig. 3 shows the ROC curves for a similar scenario to that of Fig. 2, but with different noise variances across the antennas, now given by 0, -1, 1.5 and -0.5 dB. Note that the performance of the detectors designed for uncalibrated receivers has not changed with respect to that in Fig. 2, whereas that of the detectors based on the iid noise assumption is severely degraded.

C. Asymptotic GLRT performance for finite SNR values

Although the asymptotic GLRT detector (*asympt-GLRT*) given by (23) is appealing due to its computational simplicity, it is not clear how much can be gained when the iterative scheme (*alterntng-GLRT*) is used in order to implement the exact GLRT. Fig. 4 shows the missed detection probability

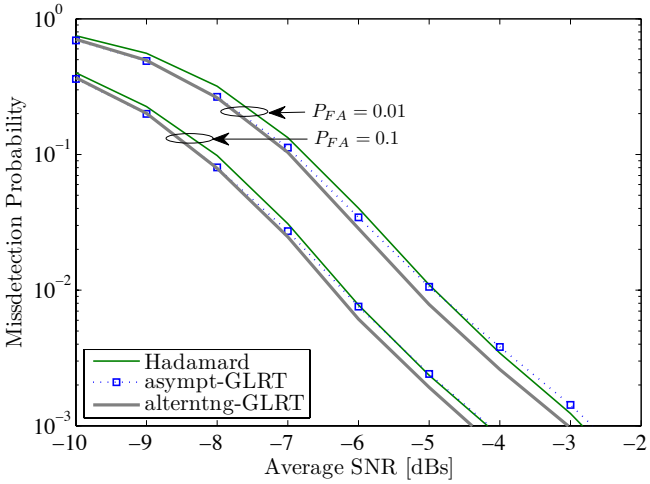

Fig. 4: Missed detection probability versus SNR for different detectors. Same scenario as in Fig. 3.

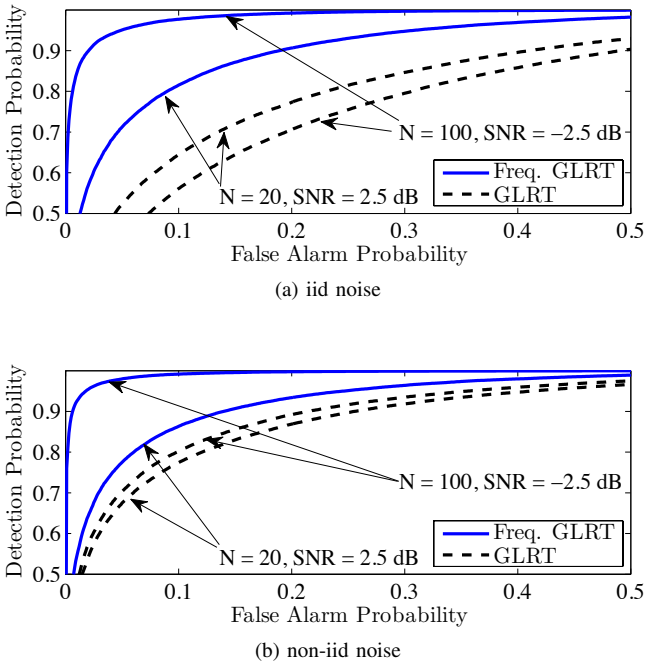

(a) iid noise

(b) non-iid noise

Fig. 5: Performance comparison of the frequency-domain GLRT against the GLRT.

of the detectors versus the SNR in a scenario similar to the previous subsection ($P = 1$, $L = 4$, $M = 128$, different noise levels at each of the antennas fixed to 0, -1, 1.5 and -0.5 dB respectively). The probability of false alarm is fixed to $P_{\text{FA}} = 0.01$ and 0.1. In Fig. 4 it is seen that for very low SNR values the asymptotic detector presents the same performance as the alternating minimization scheme. However, as the SNR increases, the GLRT outperforms the detector derived for asymptotically low SNR, as it could be expected. Note, however, that the performance loss of the asymptotic detector is rather small, and therefore it offers a good tradeoff between performance and complexity.

D. Detection performance in environments with unknown temporal structure.

Now we evaluate the performance of the proposed detectors in environments with unknown temporal structure. We consider an scenario with primary signals of rank $P = 2$, a receiver with $L = 5$ antennas, which captures $M = 5$ realizations of length $N = 100$ or $N = 20$ for the detection process. The transmitted signals use OFDM modulation, have a bandwidth of 7.61 MHz, and undergo propagation through a 5×2 uncorrelated frequency-selective channel with exponential power delay profile and delay spread 0.779 μs [35], which is fixed through the experiment. At the receiver, temporally white noises are added and the signals are sampled at 16 MHz. The SNR, defined in a frequency selective environment as

$$\text{SNR (dB)} = 10 \log_{10} \frac{\int_{-\pi}^{\pi} \text{tr}\left(\mathbf{H}\left(e^{j\theta}\right)\mathbf{H}^H\left(e^{j\theta}\right)\right)\frac{d\theta}{2\pi}}{\int_{-\pi}^{\pi} \text{tr}\left(\mathbf{\Sigma}^2\left(e^{j\theta}\right)\right)\frac{d\theta}{2\pi}}, \quad (41)$$

is given in the figures.

First, we assume iid noises. The ROC curves for the GLRT (given by (11)) and the frequency-domain GLRT for iid noises (which assumes frequency-selective channels and is given by (36)) are shown in Fig. 5a. The advantage of exploiting the temporal structure of the time series is clear. However, as can be seen in the figure, this improvement becomes smaller when the number of available samples decrease. Similar conclusions can be drawn from Fig. 5b, which shows the performance of the two GLRT detectors for uncalibrated receivers, given by (23) and (37). In this experiment the noise variance values at the different antennas were drawn from a uniform distribution in linear scale to obtain mismatches no larger than 7.5 dB.

VII. Conclusions

We have derived the GLRTs for the problem of detecting vector-valued rank-P signals when the noise covariance is assumed unknown. In particular, when the noise at each of the components is assumed iid and for uncorrelated noises non necessarily iid. As it turns out, detectors derived under the assumption of iid noises are not robust to a mismatch in noise levels across the antennas. Although the GLRT for the more challenging non-iid noise case does not admit a closed form, one can resort to numerical optimization techniques. A closed-form low SNR approximation of the GLRT has also been presented, providing a tradeoff between complexity and performance. These detectors include as particular cases several previous schemes derived either for $P = 1$ or for large P. These results have also been extended to a model considering vector-valued time series with unknown PSDs, of interest in applications with frequency selective channels and/or temporally colored noise.

All of the detectors considered here assume knowledge of the signal rank P. While this may be reasonable in some contexts, for example if the space-time coding scheme used by primary transmitters is known, there are scenarios in which P is unknown, for example if it is related to the number

of primary users simultaneously transmitting. Future research should consider estimation of P [36] and primary signal detection jointly.

APPENDIX

In this appendix, we prove the mean square convergence of the log-likelihoods, which can be seen as an extension of Whittle's likelihood [33], [34] to multivariate processes. We shall start by the conditions under which the theorem holds:

c.1 The block-Toeplitz matrices are generated by continuous symbols, i.e., each matrix block is given by the Fourier coefficients of an $L \times L$ continuous matrix function.

c.2 The power spectral matrices are positive definite.

In order to proceed, let us rewrite (31) as follows

$$\log p\left(\mathbf{z}_0, \cdots, \mathbf{z}_{M-1}; \mathcal{R}\right) = -LNM \log \pi - M \log\det\left(\mathcal{R}\right) - \sum_{m=0}^{M-1} \mathbf{z}_m^H \mathcal{R}^{-1} \mathbf{z}_m, \quad (42)$$

where $\mathcal{R}$ is given by (29). Additionally, let us introduce the block-Toeplitz matrix $\tilde{\mathcal{R}}$ which is given by

$$\tilde{\mathcal{R}} = \begin{bmatrix} \tilde{\mathbf{R}}[0] & \tilde{\mathbf{R}}[-1] & \cdots & \tilde{\mathbf{R}}[-N+1] \\ \tilde{\mathbf{R}}[1] & \tilde{\mathbf{R}}[0] & \cdots & \tilde{\mathbf{R}}[-N+2] \\ \vdots & \vdots & \ddots & \vdots \\ \tilde{\mathbf{R}}[N-1] & \tilde{\mathbf{R}}[N-2] & \cdots & \tilde{\mathbf{R}}[0] \end{bmatrix}, \quad (43)$$

where $\tilde{\mathbf{R}}[m] = \mathcal{F}^{-1}\left[\mathbf{S}^{-1}\left(e^{j\theta}\right)\right]$; and the sum of quadratic forms of the matrix $\tilde{\mathcal{R}}$

$$\sum_{m=0}^{M-1} \mathbf{z}_m^H \tilde{\mathcal{R}} \mathbf{z}_m = NM \int_{-\pi}^{\pi} \mathrm{tr}\left(\hat{\mathbf{S}}\left(e^{j\theta}\right) \mathbf{S}^{-1}\left(e^{j\theta}\right)\right) \frac{d\theta}{2\pi}. \quad (44)$$

The mean square convergence of a random variable is defined as follows (see e.g. [37]):

$$\lim_{N\to\infty} E\left[\left|\frac{1}{N}\left[\log p\left(\mathbf{z}_0, \ldots, \mathbf{z}_{M-1}; \mathcal{R}\right) - \log p\left(\mathbf{z}_0, \ldots, \mathbf{z}_{M-1}; \mathbf{S}\left(e^{j\theta}\right)\right)\right]\right|^2\right] = 0. \quad (45)$$

Substituting (31) and (42) into the left-hand side of (45), one has

$$\begin{aligned} &\lim_{N\to\infty} E\left[\left|\frac{1}{N}\left[-M\log\det\left(\mathcal{R}\right) - \sum_{m=0}^{M-1} \mathbf{z}_m^H \mathcal{R}^{-1} \mathbf{z}_m \right.\right.\right. \\ &\qquad + NM \int_{-\pi}^{\pi} \log\det\left(\mathbf{S}\left(e^{j\theta}\right)\right) \frac{d\theta}{2\pi} \\ &\qquad \left.\left.\left. - NM \int_{-\pi}^{\pi} \mathrm{tr}\left(\hat{\mathbf{S}}\left(e^{j\theta}\right) \mathbf{S}^{-1}\left(e^{j\theta}\right)\right) \frac{d\theta}{2\pi}\right]\right|^2\right] \\ &\overset{(a)}{\leq} \lim_{N\to\infty} 2M \left|\frac{1}{N}\log\det\left(\mathcal{R}\right) - \int_{-\pi}^{\pi} \log\det\left(\mathbf{S}\left(e^{j\theta}\right)\right) \frac{d\theta}{2\pi}\right|^2 \\ &\qquad + \lim_{N\to\infty} 2E\left[\left|\frac{1}{N}\sum_{m=0}^{M-1} \mathbf{z}_m^H \mathcal{R}^{-1} \mathbf{z}_m \right.\right. \\ &\qquad \left.\left. - M\int_{-\pi}^{\pi} \mathrm{tr}\left(\hat{\mathbf{S}}\left(e^{j\theta}\right) \mathbf{S}^{-1}\left(e^{j\theta}\right)\right) \frac{d\theta}{2\pi}\right|^2\right] \quad (46) \end{aligned}$$

where (a) follows from [37, Th.8, p. 287]. We shall proceed by splitting the proof in two parts, one for each term in the right-hand side of (46). It is easy to show that under c.1 and c.2, the following holds (see [38, Th. 6]

$$\lim_{N\to\infty} \frac{1}{N}\log\det\left(\mathcal{R}\right) - \int_{-\pi}^{\pi} \log\det\left(\mathbf{S}\left(e^{j\theta}\right)\right) \frac{d\theta}{2\pi} = 0. \quad (47)$$

Then, taking into account that

$$\lim_{N\to\infty} a_N = 0 \quad \Rightarrow \quad \lim_{N\to\infty} |a_N|^2 = 0, \quad (48)$$

where a_N is any sequence of real numbers, it follows that

$$\lim_{N\to\infty} 2M \left|\frac{1}{N}\log\det\left(\mathcal{R}\right) - \int_{-\pi}^{\pi} \log\det\left(\mathbf{S}\left(e^{j\theta}\right)\right) \frac{d\theta}{2\pi}\right|^2 = 0. \quad (49)$$

Now, taking into account (44), it is readily shown that

$$\begin{aligned} &\lim_{N\to\infty} E\left[\left|\frac{1}{N}\sum_{m=0}^{M-1} \mathbf{z}_m^H \mathcal{R}^{-1} \mathbf{z}_m \right.\right. \\ &\qquad \left.\left. - M\int_{-\pi}^{\pi} \mathrm{tr}\left(\hat{\mathbf{S}}\left(e^{j\theta}\right) \mathbf{S}^{-1}\left(e^{j\theta}\right)\right) \frac{d\theta}{2\pi}\right|^2\right] \\ &\qquad = \lim_{N\to\infty} E\left[\left|\frac{1}{N}\sum_{m=0}^{M-1} \mathbf{z}_m^H \left(\mathcal{R}^{-1} - \tilde{\mathcal{R}}\right) \mathbf{z}_m\right|^2\right]. \quad (50) \end{aligned}$$

We now prove that (50) converges to zero. First, we must note that it is a mean of the square of a sum of quadratic forms. Therefore, taking into account that the quadratic forms are uncorrelated and the formulas for the mean and variance of a quadratic form of a multivariate normal distribution [39], it follows that

$$\begin{aligned} &\lim_{N\to\infty} E\left[\left|\frac{1}{N}\sum_{m=0}^{M-1} \mathbf{z}_m^H \left(\mathcal{R}^{-1} - \tilde{\mathcal{R}}\right) \mathbf{z}_m\right|^2\right] \\ &\qquad = \lim_{N\to\infty} \frac{1}{N^2}\left\{M^2\left(\mathrm{tr}\left[\mathcal{R}\left(\mathcal{R}^{-1} - \tilde{\mathcal{R}}\right)\right]\right)^2 \right. \\ &\qquad \left. + 2M\mathrm{tr}\left[\mathcal{R}\left(\mathcal{R}^{-1} - \tilde{\mathcal{R}}\right)\mathcal{R}\left(\mathcal{R}^{-1} - \tilde{\mathcal{R}}\right)\right]\right\} = 0 \quad (51) \end{aligned}$$

where we have applied [38, Th. 3 and Th. 5] and (48). Therefore, (50) converges to zero, i.e.,

$$\begin{aligned} &\lim_{N\to\infty} E\left[\left|\frac{1}{N}\sum_{m=0}^{M-1} \mathbf{z}_m^H \mathcal{R}^{-1} \mathbf{z}_m \right.\right. \\ &\qquad \left.\left. - M\int_{-\pi}^{\pi} \mathrm{tr}\left(\hat{\mathbf{S}}\left(e^{j\theta}\right) \mathbf{S}^{-1}\left(e^{j\theta}\right)\right) \frac{d\theta}{2\pi}\right|^2\right] = 0. \quad (52) \end{aligned}$$

Finally, the proof follows from (49) and (52). □

ACKNOWLEDGMENTS

This work was supported by the Spanish Government's Ministerio de Ciencia e Innovación (MICINN) and the European Regional Development Fund (ERDF), under projects MULTIMIMO (TEC2007-68020-C04-02), COSIMA (TEC2010-19545-C04-03), DYNACS (TEC2010-21245-C02-02/TCM), SPROACTIVE (TEC2007-68094-C02-01/TCM), COMONSENS (CONSOLIDER-INGENIO 2010 CSD2008-00010) and FPU grant AP2006-2965.

REFERENCES

[1] J. Mitola and G. Q. Maguire Jr., "Cognitive radio: Making software radios more personal," *IEEE Pers. Comm.*, vol. 6, pp. 13–18, Aug. 1999.

[2] J. M. Peha, "Sharing spectrum through spectrum policy reform and cognitive radio," *Proc. IEEE*, vol. 97, no. 4, pp. 708–719, Apr. 2009.

[3] I. Akyildiz, W.-Y. Lee, M. Vuran, and S. Mohanty, "A survey on spectrum management in cognitive radio networks," *IEEE Comm. Magazine*, vol. 46, no. 4, pp. 40–48, Apr. 2008.

[4] D. Cabric, "Addressing the feasibility of cognitive radios," *IEEE Signal Process. Magazine*, vol. 25, no. 6, pp. 85–93, Nov. 2008.

[5] R. Tandra and A. Sahai, "SNR walls for signal detection," *IEEE J. Sel. Topics Signal Process.*, vol. 2, no. 1, pp. 4–17, Feb. 2008.

[6] O. Besson, S. Kraut, and L. L. Scharf, "Detection of an unknown rank-one component in white noise," *IEEE Trans. Signal Process.*, vol. 54, no. 7, pp. 2835–2839, Jul. 2006.

[7] A. Taherpour, M. Nasiri-Kenari, and S. Gazor, "Multiple antenna spectrum sensing in cognitive radios," *IEEE Trans. Wireless Comm.*, vol. 9, no. 2, pp. 814–823, Feb. 2010.

[8] R. López-Valcarce, G. Vazquez-Vilar, and J. Sala, "Multiantenna spectrum sensing for cognitive radio: overcoming noise uncertainty," in *Proc. Int. Work. Cognitive Inf. Process.*, Elba, Italy, Jun. 2010.

[9] P. Wang, J. Fang, N. Han, and H. Li, "Multiantenna-assisted spectrum sensing for cognitive radio," *IEEE Trans. Vehicular Tech.*, vol. 59, no. 4, pp. 1791–1800, May 2010.

[10] Y. Zeng, Y.-C. Liang, and R. Zhang, "Blindly combined energy detection for spectrum sensing in cognitive radio," *IEEE Signal Process. Lett.*, vol. 15, pp. 649–652, 2008.

[11] M. Alamgir, M. Faulkner, J. Gao, and P. Conder, "Signal detection for cognitive radio using multiple antennas," in *IEEE Int. Symp. Wireless Comm. Systems*, 2008.

[12] Y. Zeng and Y.-C. Liang, "Eigenvalue-based spectrum sensing algorithms for cognitive radio," *IEEE Trans. Comm.*, vol. 57, no. 6, pp. 1784–1793, Jun. 2009.

[13] ETSI, "Digital Video Broadcasting (DVB); Frame structure channel coding and modulation for a second generation digital terrestrial television broadcasting system (DVB-T2)," *ETSI EN 302 755*, 2009.

[14] IEEE Computer Society, "IEEE Standard 802.11n-2009. Part 11: Wireless LAN Medium Access Control (MAC) and Physical Layer (PHY) Specifications. Amendment 5: Enhancements for Higher Throughput," 2009.

[15] IEEE Computer Society and the IEEE Microwave Theory and Techniques Society, "IEEE Standard 802.16-2009. Part 16: Air Interface for Broadband Wireless Access Systems," 2009.

[16] 3GPP, "LTE Release 9," *3GPP*, 2009.

[17] D. Ramírez, J. Vía, and I. Santamaría, "Multiantenna spectrum sensing: The case of wideband rank-one primary signals," in *Proc. IEEE Sensor Array and Multichannel Signal Process. Work.*, Israel, Oct. 2010.

[18] D. Ramírez, J. Vía, I. Santamaría, and L. L. Scharf, "Detection of spatially correlated Gaussian time-series," *IEEE Trans. Signal Process.*, vol. 58, no. 10, Oct. 2010.

[19] D. Ramírez, J. Vía, I. Santamaría, R. López-Valcarce, and L. L. Scharf, "Multiantenna spectrum sensing: Detection of spatial correlation among time-series with unknown spectra," in *Proc. IEEE Int. Conf. on Acoust., Speech and Signal Process.*, Mar. 2010.

[20] J. Mauchly, "Significance test for sphericity of a normal n-variate distribution," *Ann. Math. Statist.*, vol. 11, pp. 204–209, 1940.

[21] T. J. Lim, R. Zhang, Y.-C. Liang, and Y. Zeng, "GLRT-based spectrum sensing for cognitive radio," in *Proc. Global Comm. Conf.*, 2008.

[22] R. Zhang, T. J. Lim, Y.-C. Liang, and Y. Zeng, "Multi-antenna based spectrum sensing for cognitive radios: a GLRT approach," *IEEE Trans. Comm.*, vol. 58, no. 1, pp. 84–88, Jan. 2010.

[23] S. Wilks, "On the independence of k sets of normally distributed statistical variables," *Econometrica*, vol. 3, pp. 309–325, 1935.

[24] A. Leshem and A.-J. Van der Veen, "Multichannel detection and spatial signature estimation with uncalibrated receivers," in *Proc. 11th IEEE Work. Stat. Signal Process.*, 6–8 Aug. 2001, pp. 190–193.

[25] ——, "Multichannel detection of Gaussian signals with uncalibrated receivers," *IEEE Signal Process. Lett.*, vol. 8, no. 4, pp. 120–122, Apr. 2001.

[26] A.-J. Boonstra and A.-J. Van der Veen, "Gain calibration methods for radio telescope arrays," *IEEE Trans. Signal Process.*, vol. 51, pp. 25–38, 2003.

[27] Y. Zeng and Y.-C. Liang, "Spectrum-sensing algorithms for cognitive radio based on statistical covariances," *IEEE Trans. Vehicular Tech.*, vol. 58, no. 4, pp. 1804–1815, May 2009.

[28] J. Font-Segura and X. Wang, "GLRT-based spectrum sensing for cognitive radio with prior information," *IEEE Trans. Comm.*, vol. 58, no. 7, pp. 2137–2146, Jul. 2010.

[29] K. V. Mardia, J. T. Kent, and J. M. Bibby, *Multivariate Analysis*. New York: Academic, 1979.

[30] J. R. Magnus and H. Neudecker, *Matrix differential calculus with applications in statistics and econometrics*, 2nd ed. John Wiley & Sons, 1999.

[31] T. W. Anderson, "Asymptotic theory for principal component analysis,," *The Annals of Mathematical Statistics*, vol. 34, no. 1, pp. 122–148, Mar. 1963.

[32] J. P. Burg, D. G. Luenberger, and D. L. Wenger, "Estimation of structured covariance matrices," *Proc. IEEE*, vol. 70, no. 9, pp. 963–974, 1982.

[33] P. Whittle, "Gaussian estimation in stationary time series," *Bull. Inst. Int. Statist.*, vol. 39, pp. 105–129, 1962.

[34] ——, "Estimation and information in time series analysis," *Skand. Aktuar.*, vol. 35, pp. 48–60, 1952.

[35] M. Falli, e.d., "Digital land mobile radio communications - cost 207: Final report," Luxembourg, Luxembourg, 1989.

[36] M. Chiani and M. Win, "Estimating the number of signals observed by multiple sensors," in *Proc. Int. Work. Cognitive Inf. Process.*, Elba, Italy, Jun. 2010.

[37] G. Grimmett and D. Stirzaker, *Probability and Random Processes*. Oxford Science Publications, 1992.

[38] J. Gutierrez-Gutierrez and P. M. Crespo, "Asymptotically equivalent sequences of matrices and Hermitian block Toeplitz matrices with continuous symbols: Applications to MIMO systems," *IEEE Trans. Inf. Theory*, vol. 54, no. 12, pp. 5671–5680, Dec. 2008.

[39] K. Dzhaparidze, *Parameter Estimation and Hypothesis Testing in Spectral Analysis of Stationary Time Series*. Springer-Verlag, 1986.